Biochemistry

 Volume 36, Number 31 August 5, 1997

Accelerated Publications

Changes in the Regiospecificity of Aromatic Hydroxylation Produced by Active Site Engineering in the Diiron Enzyme Toluene 4-Monooxygenase†

Jeremie D. Pikus,‡ Joey M. Studts,‡ Kevin McClay,§ Robert J. Steffan,§ and Brian G. Fox*,‡

The Institute for Enzyme Research, Graduate School and Department of Biochemistry, College of Agricultural and Life Sciences, University of Wisconsin, Madison, Wisconsin 53705, and Envirogen, Inc., Lawrenceville, New Jersey 08648

Received May 6, 1997; Revised Manuscript Received June 20, 1997⊗

ABSTRACT: *Pseudomonas mendocina* KR1 toluene 4-monooxygenase is a multicomponent diiron enzyme. The diiron center is contained in the tmoA polypeptide of the hydroxylase component [$(\alpha\beta\gamma)_2$, $M_r \approx 212$ kDa]. Product distribution studies reveal that the natural isoform is highly specific for *para* hydroxylation of toluene ($k_{cat} \approx 2\ s^{-1}$ with respect to an $\alpha\beta\gamma$ protomer), *o*-xylene ($k_{cat} \approx 0.8\ s^{-1}$), *m*-xylene ($k_{cat} \approx 0.6\ s^{-1}$), and other aromatic hydrocarbons. This degree of regioselectivity for methylbenzenes is unmatched by numerous other oxygenase enzymes. However, during the T4MO-catalyzed oxidation of *p*-xylene ($k_{cat} \approx 0.4\ s^{-1}$), 4-methyl benzyl alcohol is the major product, showing that the enzyme could catalyze either aromatic or benzylic hydroxylation with the appropriate substrate. Site-directed mutagenesis has been used to study the contributions of tmoA active site residues Q141, I180, and F205 to the regiospecificity. Isoforms Q141C and F205I yielded shifts of regiospecificity away from *p*-cresol formation, with F205I giving an ≈5-fold increase in the percentage of *m*-cresol formation relative to that of the natural isoform. The k_{cat} of purified Q141C for toluene oxidation was $\approx 0.2\ s^{-1}$. Isoform Q141C also functioned predominantly as an aromatic ring hydroxylase during the oxidation of *p*-xylene, in direct contrast to the predominant benzylic hydroxylation observed for the natural isoform, while isoform F205I gave nearly equivalent amounts of benzylic and phenolic products from *p*-xylene oxidation. Isoform I180F gave no substantial shift in product distributions relative to the natural isoform for all substrates tested. Upon the basis of a proposed active site model, both Q141 and F205 are suggested to lie in a hydrophobic region closer to the Fe_A iron site, while I180 will be closer to Fe_B. These studies reveal that changes in the hydrophobic region predicted to be nearest to Fe_A can influence the regiospecificity observed for toluene 4-monooxygenase.

Three catalytic subclasses of soluble, O_2-dependent diiron enzymes are found in aerobic organisms (Fox et al., 1994; Nordlund & Eklund, 1995). These are R2,[1] hydrocarbon hydroxylases including MMO, and stearoyl-ACP Δ^9 desaturase (Δ9D). The crystal structure of R2 revealed an 11-helix bundle polypeptide fold (Nordlund & Eklund, 1993). Glu and His residues located in four of these helices provide all of the protein ligands to the diiron center. Subsequent crystallographic studies of MMO and Δ9D revealed a closely related fold and conserved ligand spacing (Rosenzweig et

† This work was supported by grants from the Petroleum Research Foundation (ACS-PRF 28405-G4) and the NIH (GM-50853) to B.G.F. and the NSF Small Business Innovation Research Program (DMI-9460076) to R.J.S. B.G.F. is a Searle Scholar of the Chicago Community Trust (1994−1997) and a Shaw Scientist of the Milwaukee Foundation (1994−1999).

* Author to whom correspondence should be addressed. E-mail; fox@enzyme.wisc.edu. Telephone: (608) 262-9708.

‡ University of Wisconsin.

§ Envirogen, Inc.

⊗ Abstract published in *Advance ACS Abstracts,* August 1, 1997.

[1] Abbreviations: Δ9D, stearoyl-ACP Δ^9 desaturase; MMO, methane monooxygenase; PCR, polymerase chain reaction; R2, iron-containing component of aerobic ribonucleotide diphosphate reductase; T4MO, toluene 4-monooxygenase.

S0006-2960(97)01049-0 CCC: $14.00

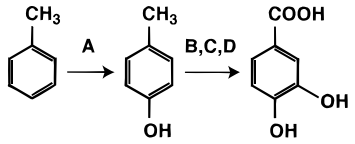

FIGURE 1: First steps in the metabolic pathway used for toluene oxidation by *P. mendocina* KR1 (Whited & Gibson, 1991a): (A) toluene 4-monooxygenase, (B) *p*-cresolmethyl hydroxylase, (C) benzaldehyde oxidoreductase, and (D) *p*-hydroxybenzoate hydroxylase.

al., 1995; Elango et al., 1997; Lindqvist et al., 1996), supporting the assignment of these enzymes to a structural family.

Additional soluble diiron enzymes include three position-specific toluene monooxygenases (Newman & Wackett, 1995; Byrne et al., 1995; Pikus et al., 1996), phenol hydroxylase (Powlowski & Shingler, 1994), alkene epoxidase (Miura & Dalton, 1995), and other acyl-ACP desaturases (Cahoon & Ohlrogge, 1994). The members of this larger group of diiron enzymes all contain the conserved metal ligand motif, hydrogen bonding to the ligands, and breaks and contacts between the α-helices. However, at positions forming the hydrophobic surface of the active site, the identities of the amino acid residues are varied. While the diiron enzymes likely utilize related redox cycles leading up to O_2 activation (Feig & Lippard, 1994; Que & Dong, 1996; Wallar & Lipscomb, 1996), it is also possible that the subsequent catalytic diversity will arise from presently undefined variations in the active site during the later stages of catalysis.

Figure 1 shows the initial steps used by *Pseudomonas mendocina* KR1 to metabolize toluene (Whited & Gibson, 1991a). The *para* hydroxylation of toluene to form *p*-cresol is catalyzed by toluene 4-monooxygenase (T4MO). The diiron hydroxylase component is assembled from the tmoA, tmoB, and tmoE polypeptides [$(\alpha\beta\gamma)_2$, $M_r \approx 212$ kDa], with the tmoA polypeptide providing the diiron motif (Pikus et al., 1996). Since toluene-grown *P. mendocina* KR1 cannot utilize *o*-cresol, *m*-cresol, or methyl catechols for growth (McClay et al., 1996), the *para* hydroxylation must proceed with high fidelity. The degree to which T4MO can produce the desired regiospecificity and the active site determinants contributing to this outcome are thus of considerable interest. Here, we report on the regiospecificity of aromatic hydroxylation by the natural isoform of the T4MO hydroxylase and on the changes in regiospecificity caused by mutation of single amino acid residues predicted to lie within the active site. These studies reveal a subtle sensitivity of the diiron active site to conservative modification and emphasize the utility of product distribution studies as probes for changes in the function of engineered hydrocarbon-oxidizing enzymes.

MATERIALS AND METHODS

Biochemical Methods. Enzyme preparation and characterization were as previously reported (Pikus et al., 1996). The Q141C isoform was prepared using these protocols. The purified hydroxylase (≈10 nmol, but adjusted for the turnover number of a given substrate or for the lower turnover number of the Q141C isoform) and the appropriate amounts of the other protein components were added to provide ≈10 μmol of total products during a 5 min assay period. The reactions were performed in Teflon-sealed 6 mL reaction vials containing 250 μL of 50 mM phosphate buffer at pH 7.5, and the aromatic substrate and NADH were added in excess. Other details of the whole-cell and purified enzyme oxidations were performed as previously reported (McClay et al., 1996; Pikus et al., 1996). Except for nitrobenzene, products were identified by comparison with retention times of standards using gas chromatography. Nitrobenzene oxidation products were determined by reverse phase HPLC. Standards for all products were from Aldrich (Milwaukee, WI).

Mutagenesis Shuttle Vector. The *tmoA* gene contains all of the codons subjected to PCR mutagenesis. Plasmid pRS184f was used as the source of this gene (Pikus et al., 1996). PCR was performed using a GeneAmp kit (Perkin-Elmer, Foster City, CA). The fidelities of the final PCR products were confirmed by nucleotide sequencing. The 1160 bp fragment obtained from digestion of pRS184f with *Eco*RI and *Bcl*I was inserted into vector pSK$^+$ (Stratagene, La Jolla, CA). This intermediate plasmid was designated pRS203. The *Bst*BI site at position 945 was removed from the *tmoA* fragment by PCR with TMOU1 (5′-atgttgcacacgctgggcaaggtt) and ENVB (5′-aagcccagatctatcaacgagcgCtcgaactg). This PCR silently changed the codon for E303 from GAA to GAG and rendered the *Bst*BI site at position 627 unique within the shuttle fragment. Clones containing mutated fragments could then be identified by restriction mapping. An amplified fragment lacking the *Bst*BI site at position 945 was digested with *Eco*RI and *Bgl*II and ligated into the similarly digested pRS203. The shuttle vector was named pRS204.

Hydroxylase Isoforms with a Mutation at Q141. Mutagenesis of the Q141 codon was accomplished with pRS204 as a template, ENV141C (5′-tgcgccatggccagttaTGcctgtttttc) or ENV141V (5′-tgcgccatggccagttaGTcctgtttttc), and ENVP3 (5′-atgttgcacacgctgggcaaggtt). The underlined nucleotides in ENV141C and ENV141V are a *Nco*I restriction site present in the native *tmoA* gene. Amplified products were digested with *Nco*I and *Bgl*II and ligated into similarly digested pRS204. Mutation of the Q141 codon caused the loss of the *Pvu*II restriction site. Restriction mapping using *Eco*RI, *Pvu*II, and *Bgl*II then yielded a single mutated fragment of 1090 bp. The correct insert was digested with *Eco*RI and *Bgl*II, ligated into similarly digested pRS184f, and used to transform *Escherichia coli* DH5α. For enzyme expression, these plasmids were maintained in *E. coli* DH5α on Luria Bertani medium supplemented with 400 μg/mL ampicillin.

Hydroxylase Isoforms with a Mutation at F205. Mutagenesis of the F205 codon was accomplished with pRS204 as a template, ENV205I (5′-tcattcgaaaccggcttcaccaacatgcagAttcttg), and ENVP3. The amplified products were digested with *Bst*BI and *Bgl*II and ligated into similarly digested pRS204. Since the shuttle fragment was modified to contain a single *Bst*BI site, restriction mapping of correctly mutated inserts using *Eco*RI, *Bst*BI, and *Bgl*II yielded two fragments from the insert. The correct insert was digested with *Eco*RI and *Bgl*II, ligated into similarly digested pRS184f, and used to transform *E. coli* DH5α.

Hydroxylase Isoform with the Mutation I180F. Mutagenesis of the I180 codon was accomplished with pRS204 as a template, TMOU1, ENV180PR (5′-cgcatcacgAccggtaaAgatgtccatc), ENV180PF (5′-gatgacatcTttaccggTcgtgatgcg), and ENVP3. The underlined nucleotides in ENV180PF and

Table 1: Products and Kinetic Parameters for the Oxidation of Aromatic Hydrocarbons by the Purified Native Isoform of Recombinant Toluene 4-Monooxygenase

substrate	products	percentage[a,b]	k_{cat}[c] (s^{-1})
toluene	*p*-cresol	96.0	2.0[d]
	m-cresol	2.8	
	o-cresol	0.4	
	benzyl alcohol	0.8	
m-xylene	2,4-dimethylphenol	97.0	0.7
	3-methyl benzyl alcohol	2.5	
	3,5-dimethylphenol	0.5	
	2,6-dimethylphenol	nd	
p-xylene	2,5-dimethylphenol	82	0.6
	4-methyl benzyl alcohol	18	
o-xylene	3,4-dimethylphenol	95	0.8
	2,3-dimethylphenol	nd	
	2-methyl benzyl alcohol	5	
benzene	phenol	100	0.8
chlorobenzene	4-chlorophenol	>95	2.2
methoxybenzene	4-methoxyphenol	>99	2.4
nitrobenzene	*p*-nitrophenol	88	2.4
	m-nitrophenol	9	
	o-nitrophenol	3	

[a] Percentage of total products determined by gas chromatography. [b] nd, not detected. [c] Maximal turnover number relative to an $\alpha\beta\gamma$ protomer in a saturated aqueous solution. Concentrations of saturated aqueous solutions of substrates are as follows (millimolar, 25 °C): toluene, 5.8; *m*-xylene, 1.5; *p*-xylene, 1.7; *o*-xylene, 1.6; benzene, 23; chlorobenzene, 4.4; methoxybenzene, 1.1; and nitrobenzene, 19.6. [d] Isoform Q141C exhibited a k_{cat} of 0.2 s^{-1} under the same experimental conditions.

ENV180PR define an *Age*I restriction site introduced by silent mutation. Primers TMOU1 and ENV180PR were used to amplify the 5′ end of the *tmoA* gene up to nucleotide 555, to change the codon for Ile180 to Phe, and to insert the *Age*I restriction site. Primers ENV180PF and ENVP3 were used to amplify the region of the *tmoA* gene from nucleotide 529 to nucleotide 1196. The two PCR products were digested with *Age*I and ligated, yielding a piece containing the I180F mutation and an adjacent *Age*I site. The combined piece was digested with *Eco*RI and *Bgl*I and inserted into similarly digested pRS204. Screening with *Eco*RI, *Age*I, and *Bgl*I then yielded two fragments. A shuttle plasmid known to contain the correct insert was digested with *Eco*RI and *Bgl*II, ligated into similarly digested pRS184f, and used to transform *E. coli* DH5α.

RESULTS

Oxidation of Toluene and Substituted Benzenes by the Natural Isoform of T4MO. Table 1 and Figure 2 show the products obtained from the oxidation of toluene by purified preparations of the natural isoform of T4MO hydroxylase. During all oxidations shown in Table 1, reaction conditions were established so that ≈10 μmol of total products was accumulated. The detection limit was ≈1 nmol (0.01% of total products), and a total overall deviation in product percentages of less than 2% was determined from three trials using different enzyme preparations. The products obtained consisted of *p*-cresol (**2a**, 96.0%), *m*-cresol (**2b**, 2.8%), *o*-cresol (**2c**, 0.4%), and benzyl alcohol (**2d**, 0.8%). No dihydroxylated products were detected. This uniquely high specificity for aromatic ring hydroxylation has likely evolved from natural constraints placed on the enzyme by the subsequent steps of the *ortho* fission pathway used by *P. mendocina* KR1 (Figure 1B−D, but particularly step B, *p*-cresolmethyl hydroxylase).

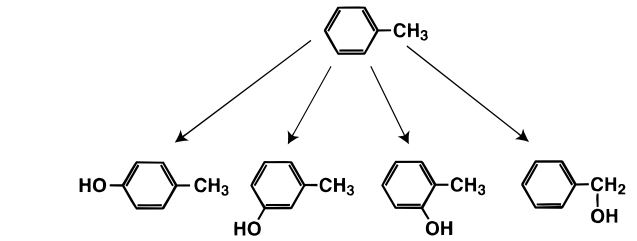

	2a	2b	2c	2d
wt	96.0	2.8	0.4	0.8
Q141C	85.0	5.0	4.0	6.0
F205I	81.0	14.5	3.5	1.0
I180F	96.7	1.2	0.2	1.9

FIGURE 2: Product distributions observed during the oxidation of toluene by the natural (wt), Q141C, I180F, and F205I isoforms of recombinant toluene 4-monooxygenase. Data for the natural and Q141C isoforms were from purified enzyme studies. Data for the I180F and F205I isoforms were from whole cell oxidations. Amounts of purified enzymes or cell cultures were adjusted so that ≈10 μmol of total products was obtained from all oxidations. The product distributions were determined by averaging the results from oxidations performed with three different enzyme or whole cell preparations. The total deviation in product ratios was ≈2%; the minor products were reproducibly detected in all replicate assays.

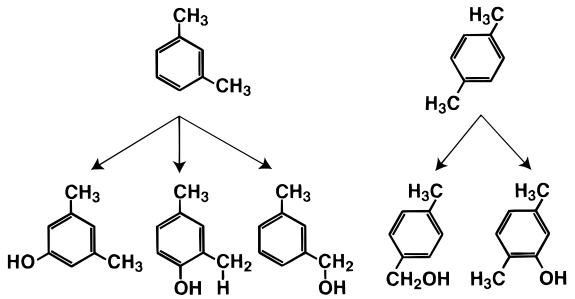

	3a	3b	3c	3d	3e
wt	0.3	97.4	2.2	82	18
Q141C	~0.1	88.3	11.7	22	78
F205I	~0.1	88.4	11.6	42	58
I180F	0.6	90.6	8.8	89	11

FIGURE 3: Product distributions observed during the oxidation of *m*-xylene and *p*-xylene by the natural (wt), Q141C, I180F, and F205I isoforms of recombinant toluene 4-monooxygenase. Reaction systems were as in Figure 2.

Table 1 also summarizes the product distributions obtained from oxidations of other substituted benzenes by the purified enzyme. For chlorobenzene (deactivating for electrophilic substitution, *ortho*, *para* directing), methoxybenzene (activating, *ortho*, *para* directing), and nitrobenzene (deactivating, *meta* directing), the predominant product was always hydroxylated in a *para* position relative to the ring substituent. Since a substantial fraction of *meta* functionalized product (85−93%) would be expected from a nonenzymatic electrophilic addition to nitrobenzene in the absence of steric effects (Taylor, 1990), the formation of ≈90% of *p*-nitrophenol during the T4MO-catalyzed hydroxylation provides strong supporting evidence for the importance of steric contributions from the T4MO active site.

The regiospecificity for *para* aromatic ring hydroxylation was also maintained during the oxidation of two xylene isomers by the natural isoform. During the oxidation of *o*-xylene, 3,4-dimethylphenol was the major product (Table 1, >95% yield), and this reaction was not investigated further. During the oxidation of *m*-xylene (Figure 3), 2,4-dimethylphenol was likewise the major product (**3b**, 97.4%), with 3-methyl benzyl alcohol (**3c**) and 3,5-dimethylphenol

Table 2: Comparison of Selected Active Site Residues in Methane Monooxygenase Hydroxylase[a] and Residues Predicted for Toluene Monooxygenases[b]

MMO	T4MO[c]	T3MO[d]	T2MO[e]	mutations[f]
L110	I100	I100	V106	
A117	A107	A107	A113	
C151	**Q141**	Q141	E147	Q141C, Q141V
F188	F176	F176	F181	
G191	I179	L179	D184	
F192	**I180**	F180	A185	I180F
L204	L192	L192	V197	
G208	F196	F196	F201	
T213	T201	T201	T206	
I217	**F205**	F205	F210	F205I
F236	I224	I224	G229	
I239	I227	I227	A232	

[a] MMO active site residues identified by X-ray crystallography (Rosenzweig et al., 1995; Elango et al., 1997). [b] Toluene monooxygenase residues determined by primary sequence alignments (Fox et al., 1994; Johnson & Olsen, 1995). [c] T4MO residues subjected to mutagenesis are in bold typeface. [d] Toluene 3-monooxygenase from *Pseudomonas pickettii* PK01. [e] Toluene 2-monooxygenase from *Pseudomonas* sp. strain JS150. [f] Mutations produced for this study.

(**3a**) detected as minor products. The one other possible isomeric phenol, 2,6-dimethylphenol, was not detected. For *m*-xylene, the total overall deviation in product percentages was again ≈2% from three trials using different preparations of the enzyme. In contrast to the *o*- and *m*-xylene results, the major product obtained from the oxidation of *p*-xylene (Figure 3) was 4-methyl benzyl alcohol (**3d**, 82%). Thus, with the appropriate orientation of methyl groups, the enzyme was capable of benzylic hydroxylation in high yield.

Table 1 contains the kinetic constants for oxidations using the purified natural isoform. Under conditions where the other protein components were present in the optimal amounts, and where NADH, O_2, and the substrate were present at a saturating concentration, the k_{cat} for toluene was 2.0 s^{-1} at 25 °C relative to an $\alpha\beta\gamma$ protomer; the turnover numbers for chlorobenzene, methoxybenzene, and nitrobenzene were similar. For *m*-xylene, the k_{cat} was 0.7 s^{-1}, while for *p*-xylene, the k_{cat} was 0.6 s^{-1}; similar turnover numbers were obtained for *o*-xylene and benzene. For all of the substituted benzenes shown in Table 1, the natural isoform had K_m values of ≈10−30 μM.[2] Thus, the apparent k_{cat}/K_m values for these varied substrates differed by only 10−30-fold, in contrast to the ≈10^4-fold differences in reactivity observed in chemical electrophilic substitution reactions (Taylor, 1990).

Functional Model for the T4MO Hydroxylase Active Site. The crystal structure of MMO has revealed that ≈50 residues from five α-helices produce the active site region (Rosenzweig et al., 1995; Elango et al., 1997). A subset of these residues are shown in Table 2, along with the comparable residues predicted for three position-specific toluene monooxygenases. Using this information, we developed a model for the T4MO hydroxylase active site shown in Figure 4. This model consists of two hydrophobic shells surrounding the diiron center. One shell, containing Q141 and F205, would be closer to Fe_A, while the other shell, containing I180, would be closer to Fe_B.

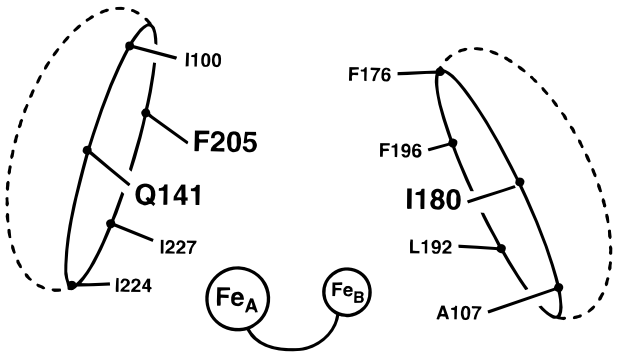

FIGURE 4: Model for two hydrophobic shells in the active site of toluene 4-monooxygenase. The proposed positions for the amino acids were determined from sequence alignments and the MMO crystal structures described in the text.

Active site mutations in the T4MO hydroxylase generated on the basis of this model are listed in Table 2. The potential contribution of C151 to the MMO catalytic mechanism has been previously proposed (Nordlund et al., 1992; Feig & Lippard, 1994: Rosenzweig et al., 1995). Thus, we were interested in the catalytic properties of T4MO isoforms mutated at this position and have generated Q141C and Q141V. In addition, T4MO hydroxylase residues I180 and F205 occupy what are clearly hydrophobic positions in all other diiron hydroxylases. Since variations of these residues could produce changes in the shape of the active site, we were interested in whether these residues contribute to the regiospecificity.

Survey of Catalytic Properties of T4MO Mutant Isoforms. Recombinant hosts containing the natural T4MO hydroxylase oxidize indole, leading to accumulation of the blue dye indigo (Yen et al., 1991). This reaction provided a useful initial functional screen for catalytic activity. By the criteria of time-dependent appearance of blue color on agar plates or in liquid medium culture, all mutated isoforms described here retained catalytic activity. Moreover, both purified enzyme systems (natural isoform and Q141C) and induced bacterial cells in shaken flask culture gave the same product distributions for toluene and xylene oxidations within experimental error. This result shows that the recombinant host could not metabolize either cresols or benzyl alcohol on the time scale of these experiments and established the validity of using whole-cell preparations for some product determinations.

The product distributions from the oxidation of toluene, *m*-xylene, and *p*-xylene by the purified natural isoform of T4MO hydroxylase (Figures 2 and 3) provide useful benchmarks for evaluating the catalytic properties of T4MO isoforms obtained from mutagenesis. For direct comparison, the products obtained from oxidations catalyzed by these mutant isoforms are also shown in Figures 2 and 3. In summary, the Q141C- and F205I-catalyzed oxidations of toluene (Figure 2) and *p*-xylene (Figure 3) yielded the largest changes in the product distributions relative to those obtained from the natural isoform. For isoform I180F and for oxidation of *m*-xylene by all isoforms, the predominant oxidation product remained a phenol with O-atom insertion *para* to a methyl substituent. Further analysis of the catalytic

[2] The errors in K_m values arise from a combination of the relatively high affinity of the enzyme for these substrates, the limited sensitivity of the assay methods, and the turnover number of the enzyme complex. At low substrate concentrations, the assumption of a large excess of substrate relative to the enzyme is not strictly true. Moreover, the fraction of uncoupled turnover relative to that observed under conditions of saturating hydrocarbons appears to vary in a complex manner as the substrate concentration becomes limiting (J. M. Studts, J. D. Pikus, and B. G. Fox, unpublished results).

properties and the product distributions of these isoforms are provided below.

Glutamine 141. Residue Q141 aligns with Y122 of *E. coli* R2 (Nordlund & Eklund, 1993), C151 of MMO (Rosenzweig et al., 1995), and L189 of Δ9D (Lindqvist et al., 1996). Y122 is converted by O_2-dependent single turnover of the diferrous center into a catalytically essential free radical (Tong et al., 1996). Since the corresponding position in MMO is C151, a thiyl radical intermediate has been invoked in mechanisms for the methane hydroxylation reaction (Nordlund et al., 1992; Feig & Lippard, 1994). However, since other diiron hydroxylases most likely have either Gln or Glu at this position (Fox et al., 1994; Johnson & Olsen, 1995), the chemical nature of a putative catalytic radical would be quite different. In the T4MO complex, both Q141C and Q141V oxidize toluene and indole, proving that the identity of the residue at this position in the T4MO active site is not absolutely essential for hydroxylation. Further characterizations of the regiospecificity of the Q141V isoform were not undertaken because the rate of toluene oxidation was ≈100-fold slower than that of the natural isoform. The purified Q141C isoform also had a K_m value of ≈10−30 μM for toluene oxidation, which is quite similar to that of the natural isoform. However, the maximal turnover number for the Q141C isoform was decreased 10-fold to 0.2 s^{-1} at 25 °C.

Figures 2 and 3 compare the percentage of product yields from the oxidation of toluene, *m*-xylene, and *p*-xylene by purified Q141C with those of the natural isoform and other mutant isoforms. During the Q141C-catalyzed oxidation of toluene, the yield of *p*-cresol was slightly decreased (**2b**, ≈85%), while the remaining material balance was distributed nearly equally between the other three possible products. During the oxidation of *m*-xylene, Q141C yielded an ≈6-fold increase in 3-methyl benzyl alcohol (**3c**, 11.7%) relative to the native isoform, while 3,5-dimethylphenol (**3a**) was detectable at a trace level.

Notably, during the Q141C-catalyzed oxidation of *p*-xylene, the major product was 2,5-dimethylphenol (**3e**, 78%). Thus, for *p*-xylene, a substrate where only two oxidation products are possible, the active site change Q141C produced a nearly complete switch in the product distribution from benzylic to aromatic hydroxylation.

Phenylalanine 205 and Isoleucine 180. The inner surface of the diiron active site is formed by a number of hydrophobic residues (Nordlund & Eklund, 1993; Rosenzweig et al., 1995; Lindqvist et al., 1996) that have been proposed to sequester oxidative intermediates from adventitious quenching by water and protons. Furthermore, hydrophobic substrates such as toluene are likely oriented within this surface to provide the regiospecificity of the natural enzyme (Figure 2). At one hydrophobic position nearest to Fe_A in the active site, all toluene monooxygenases contain Phe residues (F205 in T4MO) while MMO has I217. In order to match the amino acid residue found in MMO, we produced the F205I isoform. Figure 2 shows that this isoform had an altered regiospecificity for toluene oxidation but still yielded a predominant fraction of *p*-cresol (**2a**, 81.0%). The second major product, *m*-cresol (**2b**, 14.5%), was produced in an ≈5-fold higher level than that observed from the natural isoform. During the oxidation of *m*-xylene (Figure 3), F205I yielded an ≈6-fold increase in the percentage of 3-methyl benzyl alcohol (**3c**, 11.6%) relative to the native isoform (**3c**, 2%), while 3,5-dimethylphenol was detectable at a trace level. Within experimental error, this product distribution was identical to that obtained from Q141C. However, during the F205I-catalyzed oxidation of *p*-xylene (Figure 3), 4-methyl benzyl alcohol (**3d**, 42%) and 2,5-dimethylphenol (**3e**, 58%) were obtained in nearly equivalent quantities. This again represents a substantial deviation relative to the predominant benzylic hydroxylation observed for the natural isoform and the predominant aromatic hydroxylation observed for Q141C.

Nucleotide sequence analyses have shown that toluene 3-monooxygenase and T4MO hydroxylase are highly homologous proteins (Byrne et al., 1995). Table 2 shows that the amino acid sequence of these natural enzymes may differ only at positions 179 and 180 within the active site. These positions are predicted to be closest to the Fe_B site. Since Ile and Phe provided the largest volume difference, we investigated the possibility that the single mutation I180F could switch the regiospecificity between *para* and *meta* hydroxylation of toluene. However, the product distributions determined for I180F were nearly identical to that of the natural isoform for all substrates tested (Figures 2 and 3).

DISCUSSION

The product distributions reported here confirm that the natural isoform of T4MO hydroxylase tightly controls the hydroxylation regiospecificity. For toluene, the percentage of the major product *p*-cresol (**2a**, 96.4%) was nearly identical to that previously determined using [^{14}C]toluene (96.2%) (Whited & Gibson, 1991b). In order to produce this regiospecificity, the interior surface of the enzyme active site must not only optimize the orientation of the methyl group and the aromatic ring relative to the oxidizing intermediate but also effectively limit access to alternative binding configurations during the lifetime of the oxidation reaction. This tightly controlled regiospecificity is underscored by the products obtained from the oxidation of *m*-xylene, where despite the fact that the *para* aromatic C−H bond (∼110 kcal/mol) and the adjacent benzylic C−H bond (∼85 kcal/mol) are separated by ≈2.5 Å, a nearly complete specificity for aromatic hydroxylation is retained (**3b**).

Regiospecificity of Other Oxygenase Complexes. Enzymes, including ammonia monooxygenase (Vannelli & Hooper, 1995), chloroperoxidase (Miller et al., 1995), cytochrome P450 (Hanzlik & Ling, 1993; Tassaneeyakul et al., 1996), methane monooxygenase (Dalton, 1980), and xylene monooxygenase (Wubbolts et al., 1994), also hydroxylate alkylbenzenes. These enzymes share the ability to generate potent oxidizing intermediates and yield products consistent with electrophilic, radical-like reaction pathways. Also in common, the majority products (70−100% of total) are benzyl alcohols while the phenolic products studied more often either are obtained in relatively minor amounts or are not detected. Upon consideration of this preference for benzylic hydroxylation, enzymes like T4MO that are specialized for aromatic ring monooxygenation are relatively rare. However, the ability of T4MO to catalyze the benzylic hydroxylation of *p*-xylene also shows that there is no absolute mechanistic barrier to aliphatic hydroxylation. This reactivity is consistent with other similarities between T4MO and MMO, although methane and other small aliphatic hydrocarbons are apparently not oxidized by T4MO (McClay et al., 1996).

Site-directed mutagenesis has been extensively used to study P450s (Poulos, 1995). Single amino acid changes in $P450_{BM-3}$ produced a shift from ω-1 to ω hydroxylation for laurate oxidation (Oliver et al., 1997) and modified the regiospecificity of $P450_{2a5}$ for hydroxylation of dehydroepiandosterone (Uno et al., 1997). In contrast, single amino acid changes in $P450_{CAM}$ had a small effect on the regiospecificity of camphor oxidation, possibly because of the highly complementary fit of the natural substrate in the active site (Sligar et al., 1991). Single amino changes Y96A or Y96F did substantially increase the ability of $P450_{CAM}$ to oxidize alternative substrates such as linear and branched chain alkanes, however (Stevenson et al., 1996). Since these alkanes are normally poor substrates for $P450_{CAM}$, the increased catalytic activity was proposed to reflect a change in the hydrophobicity of the active site that increased the substrate affinity. Moreover, for Y96F, the yield of 2-methyl-2-pentanol from 2-methylpentane was increased 1.3-fold from 60 to 78% of total products, suggesting an incremental optimization of one binding orientation.

Functional Properties of the T4MO Active Site Model. The numerous biochemical, catalytic, and spectroscopic similarities between T4MO and MMO, along with the crystal structures of the latter, provide the basis for the T4MO active site model shown in Figure 4. In this model, two shells of predominantly hydrophobic amino acids form the active site surface. Upon consideration of the larger family of bacterial diiron hydroxylases, these hydrophobic amino acids exhibit the greatest variability, while residues assembling the diiron center are conserved.

Because of the introduction of changes to amino acid residues in three different positions in the hydrophobic shells shown in Figure 4, changes in product distributions were observed that apparently arise from a reshaping of this interior surface. The most dramatic changes in toluene product distribution were observed with Q141C and F205I, and these changes could be amplified by using *p*-xylene as an alternative substrate. Notably, Q141 and F205 are predicted to be on the same side of the active site, and would be located in proximity to Fe_A. In contrast, I180 is predicted to be nearer to Fe_B and isoform I180F yielded essentially no change in any of the product distributions when compared to those of the natural isoform. On the basis of these studies, the hydrophobic surface surrounding the Fe_A site appears to influence the substrate orientation in the T4MO hydroxylase. This conclusion is in accord with the alignment of Q141 of the T4MO hydroxylase with Y122 of *E. coli* R2 (Nordlund & Eklund, 1993), since Y122 is converted by an O_2-dependent reaction to a stable free radical (Sjöberg et al., 1978). The differential contribution of the two proposed hydrophobic pockets based on changes in regiospecificity is also consistent with spectroscopic studies that indicate a structural inequivalence of the metal sites in reactive diiron intermediates (Liu et al., 1994; Burdi et al., 1996; Sturgeon et al., 1996) and with mechanisms that invoke functional differences of the iron atoms at later stages in the catalytic cycle (Wallar & Lipscomb, 1996; Valentine et al., 1997).

Contributions of Selected Amino Acid Residues in Catalysis. The ability of synthetic diiron model complexes to perform hydroxylation reactions has provided strong evidence for the ability of the diiron center to function alone in this chemistry (Stassinopoulos & Caradonna, 1990; Leising et al., 1993). However, since glycyl, thiyl, tryptophanyl, and tyrosyl radicals are documented participants in enzymatic oxidation reactions (Frey, 1990), an exhaustive consideration of potential hydrocarbon oxidation mechanisms would by necessity include such intermediates. On the basis of radical stabilities decreasing in the order of cysteinyl > glutaminyl ≫ valyl and on the basis of the observed catalytic activity of Q141, Q141C, and Q141V, we conclude that an amino acid radical at position 141 is not required during the toluene hydroxylation reaction. Alternatively, the product distributions of Figures 2 and 3 suggest that Q141 has an important role in forming the toluene-selective shape of the active site. This conclusion is consistent with the overall similarity of k_{cat}/K_m for the natural isoform and purified Q141C, which differ by only ∼10-fold.

For all substrates, the overall k_{cat}/K_m values differed by 10−30-fold. This is consistent with the nonselective, highly energetic nature of the oxidant. In each of the reactions studied, a single substrate was oxidized to a distribution of products, and this distribution most likely reflects a difference in microscopic k_{cat}/K_m values. For the illustrative case of *p*-xylene, which can yield only two products, the overall $k_{cat}/K_m \approx 0.6/20 \approx 0.03\ \mu M^{-1}\ s^{-1}$ which would yield microscopic k_{cat}/K_m values of 0.82 (0.03) for formation of **3d** and 0.18 (0.03) for formation of **3e**. Alternatively, the distribution could represent partitioning of the substrate between several conformations within the active site during the lifetime of the oxidation reaction.

Conclusions. These studies have established the hydroxylation regiospecificity of the diiron enzyme T4MO hydroxylase and have revealed correlations between several amino acid positions and the regiospecificity. The ability to generate catalytically distinct oxygenase isoforms by conservative mutation within the predicted active site region demonstrates the overall robustness of the diiron hydroxylase active site and suggests that the α-helical bundle containing this active site will provide a useful scaffold upon which further modifications can be engineered.

ACKNOWLEDGMENT

We thank Dr. G. Zylstra (Center for Agricultural Molecular Biology, Rutgers University) for help in performing the nucleotide sequencing analysis and Dr. G. Whited (Genecor International) for helpful discussions about the product distributions observed with the natural isoform.

REFERENCES

Burdi, D., Sturgeon, B. E., Tong, W. H., Stubbe, J., & Hoffman, B. M. (1996) *J. Am. Chem. Soc. 118*, 281−282.

Byrne, A. M., Kukor, J. J., & Olsen, R. H. (1995) *Gene 154*, 65−70.

Cahoon, E. B., & Ohlrogge, J. B. (1994) *Plant Physiol. 104*, 827−837.

Dalton, H. (1980) *Adv. Appl. Microbiol. 26*, 71−87.

Elango, N., Radhakrishnan, R., Froland, W. A., Wallar, B. J., Earhart, C. A., Lipscomb, J. D., & Ohlendorf, D. H. (1997) *Protein Sci. 6*, 556−568.

Feig, A., & Lippard, S. J. (1994) *Chem. Rev. 94*, 759−805.

Fox, B. G., Shanklin, J., Ai, J., Loehr, T. M., & Sanders-Loehr, J. (1994) *Biochemistry 33*, 12776−12786.

Frey, P. A. (1990) *Chem. Rev. 90*, 1343−1357.

Hanzlik, R. P., & Ling, K.-H. J. (1993) *J. Am. Chem. Soc. 115*, 9363−9370.

Johnson, G. R., & Olsen, R. H. (1995) *Appl. Environ. Microbiol. 61*, 3336−3346.

Leising, R. A., Kim, J., Pérez, M. A., & Que, L., Jr. (1993) *J. Am. Chem. Soc. 115*, 9524−9530.
Lindqvist, Y., Huang, W., Schneider, G., & Shanklin, J. (1996) *EMBO J. 15*, 4081−4092.
Liu, K. E., Wang, D., Huynh, B. H., Edmondson, D. E., Salifoglou, A., & Lippard, S. J. (1994) *J. Am. Chem. Soc. 116*, 7465−7466.
McClay, K., Fox, B. G., & Steffan, R. J. (1996) *Appl. Environ. Microbiol. 62*, 2716−2722.
Miller, V. P., Tschirret-Guth, R. A., & Ortiz de Montellano, P. R. (1995) *Arch. Biochem. Biophys. 319*, 333−340.
Miura, A., & Dalton, H. (1995) *Biosci., Biotechnol., Biochem. 59*, 853−859.
Newman, L. M., & Wackett, L. P. (1995) *Biochemistry 34*, 14066−14076.
Nordlund, P., & Eklund, H. (1993) *J. Mol. Biol. 232*, 123−164.
Nordlund, P., & Eklund, H. (1995) *Curr. Opin. Struct. Biol. 5*, 758−766.
Nordlund, P., Dalton, H., & Eklund, H. (1992) *FEBS Lett. 307*, 257−262.
Oliver, C. F., Modi, S., Sutcliffe, M. J., Primrose, W. U., Lian, L. Y., & Roberts, G. C. (1997) *Biochemistry 36*, 1567−1572.
Pikus, J. D., Studts, J. M., Achim, C., Kauffmann, K. E., Münck, E., Steffan, R. J., McClay, K., & Fox, B. G. (1996) *Biochemistry 35*, 9106−9119.
Poulos, T. L. (1995) *Curr. Opin. Struct. Biol. 5*, 767−774.
Powlowski, J., & Shingler, V. (1994) *Biodegradation 5*, 219.
Que, L., Jr., & Dong, Y. (1996) *Acc. Chem. Res. 29*, 190−196.
Rosenzweig, A. C., Nordlund, P., Takahara, P. M., Frederick, C. A., & Lippard, S. J. (1995) *Chem. Biol. 2*, 409−418.
Sjöberg, B.-M., Reichard, P., Gräslund, A., & Ehrenberg, A. (1978) *J. Biol. Chem. 253*, 6863−6865.
Sligar, S. G., Filipovic, D., & Stayton, P. S. (1991) *Methods Enzymol. 206*, 31−49.
Stassinopoulos, A., & Caradonna, J. P. (1990) *J. Am. Chem. Soc. 112*, 7071−7073.
Stevenson, J.-A., Westlake, A. C. G., Whittock, C., & Wong, L.-L. (1996) *J. Am. Chem. Soc. 118*, 12846−12847.
Sturgeon, B. E., Burdi, D., Chen, S., Huynh, B.-H., Edmondson, D. E., Stubbe, J., & Hoffman, B. M. (1996) *J. Am. Chem. Soc. 118*, 7551−7557.
Tassaneeyakul, W., Birkett, D. J., Edwards, J. W., Veronese, M. E., Tassaneeyakul, W., Tukey, R. H., & Miners, J. O. (1996) *J. Pharmacol. Exp. Ther. 276*, 101−108.
Taylor, R. (1990) *Electrophilic Aromatic Substitution*, John Wiley & Sons, New York.
Tong, W. H., Chen, S., Lloyd, S. G., Edmondson, D. E., Huynh, B.-H., & Stubbe, J. (1996) *J. Am. Chem. Soc. 118*, 2107−2108.
Uno, T., Mitchell, E., Aida, K., Lambert, M. H., Darden, T. A., Pedersen, L. G., & Negishi, M. (1997) *Biochemistry 36*, 3193−3198.
Valentine, A. M., Wilkinson, B., Liu, K. E., Komar-Panicucci, S., Priestly, N. D., Williams, P. D., Morimoto, H., Floss, H. G., & Lippard, S. J. (1997) *J. Am. Chem. Soc. 119*, 1818−1827.
Vannelli, T., & Hooper, A. B. (1995) *Biochemistry 34*, 11743−11749.
Wallar, B. J., & Lipscomb, J. D. (1996) *Chem. Rev. 96*, 2625−2657.
Whited, G. M., & Gibson, D. T. (1991a) *J. Bacteriol. 173*, 3017−3020.
Whited, G. M., & Gibson, D. T. (1991b) *J. Bacteriol. 173*, 3010−3016.
Wubbolts, M. G., Reuvekamp, P., & Witholt, B. (1994) *Enzyme Microb. Technol. 16*, 608−615.
Yen, K.-M., Karl, M. R., Blatt, L. M., Simon, M. J., Winter, R. B., Fausset, P. R., Lu, H. S., Harcourt, A. A., & Chen, K. K. (1991) *J. Bacteriol. 173*, 5315−5327.

BI971049T